Experimental Validation of an Electrical Equivalent Model for MEMS Coriolis Vibratory Gyroscopes

Madan Parajuli[1], Hamza Abdelli[1], Guillermo Sobreviela[1], Ashwin Seshia[1,2]
Email: {mparajuli, habdelli, gsobreviela}@silicong.com, aas41@cam.ac.uk
[1] Silicon Microgravity Ltd., Cambridge Innovation Park, Waterbeach, Cambridge, UK
[2] Nanoscience Centre, Department of Engineering, University of Cambridge, Cambridge, UK

***Abstract*—This paper presents a linear electrical equivalent model for a MEMS Coriolis Vibratory Gyroscope (CVG). The MEMS CVG is represented as a 4-port (2-input ports and 2-output ports) system. This model includes the system dependence with respect to the bias voltage, tuning electrode voltages, and applied rotational input. The model is validated through measurements of the response in open loop at zero rate and during operation on a rotary table conducted on a fabricated MEMS gyroscope prototype. The results from the model and the experiments are compared and discussed in this paper.**

Keywords—MEMS, Gyroscope, Modelling

I. Introduction

MEMS Coriolis vibratory gyroscopes operate on the principle of coupling between two or more vibratory modes of a micromachined structure in the presence of an applied external rotation [1]. The MEMS element is closely integrated with front-end/signal conditioning electronics and the design optimization relies on the development of accurate models of the integrated system. This work moves away from traditional control loop models based on state-space representation and from models such as VerilogA, favouring electrical equivalent models which enable physical intuition in the design optimization process. In the case of coupled resonator systems such as MEMS gyroscopes, suitable approaches to implement the elastic, Coriolis and other coupling terms must be implemented. This paper proposes an electrical equivalent model for MEMS CVGs that can also be extended to coupled resonator systems closely integrated with interface and control circuitry.

II. Device

The device-under-test in this study is a vacuum packaged micromachined disk gyroscope fabricated in a (100) single crystal silicon (SCS) substrate using a silicon-on-insulator (SOI) MEMS process employing wafer-level vacuum encapsulation [2]. The top view and perspective view of the device are presented in Fig. 1. The key mechanical features of this device include a ring supported by a quatrefoil suspension system on the central anchor [3]. The quatrefoil suspension system consists of spiral flexures winding outward from the central anchor to the ring in both clockwise and anti-clockwise directions. These design features minimize thermoelastic damping and anchor loss leading to a quality factor of over a million for the secondary elliptical modes (Fig. 2). The external part of the ring is surrounded by 24 identical electrodes separated by a capacitive gap. The inner part of the ring is surrounded by 12 electrodes.

The sensor die is mounted on the front-end printed circuit board (PCB). The electronics is housed in a custom-built module [4]. The input electrode corresponding to each degenerate mode is actuated by a sinusoidal signal generated by the DAC output of a Digital Resonance Tracker Unit (DRTU). The output signal from each mode is amplified by a transimpedance amplifier (TIA). The DRTU digitizes the TIA output. A Field Programmable Gate Array (FPGA) based system is used for resonance tracking with the option to implement three control loops: automatic gain control (AGC), force-to-rebalance (FTR) and quadrature nulling. Electrical packaging of the device is achieved by direct wire bonding of associated bond pads to the corresponding pads on the PCB.

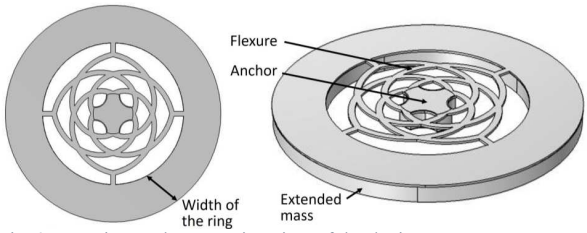

Fig. 2. Top view and perspective view of the device.

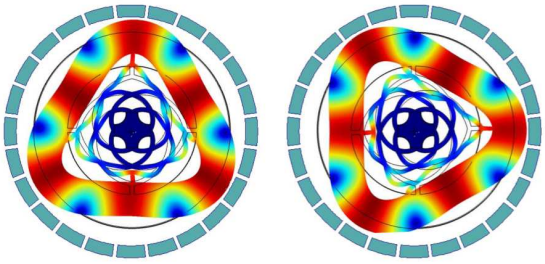

Fig. 1. Arrangement of electrodes to the drive and the sense secondary degenerate modes of the device illustrated via finite element simulation.

III. Electrical Equivalent Model

The electrical equivalent model is based on the parallelism between the electromechanical model of the MEMS resonator and electrical equivalent networks [5-7]. In this work, the describing system dynamics for the drive mode resonator (with subindex x) and sense mode resonator (with subindex y) through cross-coupling terms (subscripts xy, yx) are:

$$\begin{aligned} m_x\ddot{x} + \gamma_x\dot{x} + k_x x &= F_x + 2m_c\Omega_z\dot{y} - \gamma_{yx}\dot{y} - k_{yx}y \\ m_y\ddot{y} + \gamma_y\dot{y} + k_y y &= F_y - 2m_c\Omega_z\dot{x} - \gamma_{xy}\dot{x} - k_{xy}x \end{aligned} \quad (1)$$

where x and y are the motional position of the drive and the sense mode; m, γ and k are respectively the effective mass, the damping factor, and the effective spring constant; Ω_z is the rate of rotation applied about an axis normal to the plane of modal vibration; F_x and F_y are the external forces to drive the two modes. The terms $2m_c\Omega_z\dot{x}$ and $2m_c\Omega_z\dot{y}$ are the rotation induced Coriolis force terms. The γ_{yx}, k_{yx}, γ_{xy} and k_{xy} are the cross-coupling terms which cause the modes to interact even in the absence of the Coriolis coupling.

The conversion of lumped mass-spring-damper coupled resonators into electrical equivalent circuit models takes advantage of the analogies across the energy domains. Since the motional currents (I_{mx}, I_{my}) are related to the velocity terms $(\dot{x}, \dot{y})$, multiplied by an electromechanical transduction coefficient, the electrical equivalent of (1) can be rewritten as:

$$\begin{aligned} L_{mx}\frac{\partial I_{mx}}{\partial t} + R_{mx}I_{mx} + \frac{1}{C_{mx}}\int I_{mx}\partial t \; &= V_{inx} \\ + R_{mcy}\Omega_z I_{my} - R_{myx}I_{my} - \frac{1}{C_{myx}}\int I_{my}\partial t & \\ L_{my}\frac{\partial I_{my}}{\partial t} + R_{my}I_{my} + \frac{1}{C_{my}}\int I_{my}\partial t \; &= V_{iny} \\ -R_{mcx}\Omega_z I_{mx} - R_{mxy}I_{mx} - \frac{1}{C_{mxy}}\int I_{mx}\partial t & \end{aligned} \quad (2)$$

where V_{inx} and V_{iny} are the drive voltages of the drive and of the sense mode, $L_{mx}\frac{\partial I_{mx}}{\partial t} + R_{mx}I_{mx} + \frac{1}{C_{mx}}\int I_{mx}\partial t$ (RLC_1) and $L_{my}\frac{\partial I_{my}}{\partial t} + R_{my}I_{my} + \frac{1}{C_{my}}\int I_{my}\partial t$ (RLC_2) represent the drive and sense mode's resonators; $R_{mcy}\Omega_z I_{my}$ and $R_{mcx}\Omega_z I_{mx}$ represent the Coriolis coupling from sense to drive mode (V_{CORx}) and from drive to sense mode (V_{CORy}) respectively; $R_{myx}I_{my} - \frac{1}{C_{myx}}\int I_{my}\partial t$ and $-R_{mxy}I_{mx} - \frac{1}{C_{mxy}}\int I_{mx}\partial t$ represent capacitive and resistive coupling from the sense mode to the drive mode (V_{MCx}) and the drive mode to the sense mode (V_{MCy}). Equation (2) can be simplified in the Laplace space as:

$$\begin{pmatrix} V_{inx} \\ V_{iny} \end{pmatrix} = \begin{pmatrix} RLC_{mx} & RC_{xy} - R_{cy}\Omega_z \\ RC_{yx} - R_{cx}\Omega_z & RLC_{my} \end{pmatrix}\begin{pmatrix} I_{mx} \\ I_{my} \end{pmatrix} \quad (3)$$

where

$$RLC_{mx} = R_{mx} + L_{mx}s + \frac{1}{C_{mx}s},$$
$$RLC_{my} = R_{my} + L_{my}s + \frac{1}{C_{my}s},$$
$$RC_{xy} = R_{xy} + \frac{1}{C_{mxy}s} \text{ and}$$
$$RC_{yx} = R_{yx} + \frac{1}{C_{myx}s}$$

Equation (3) can be written as:

$$\begin{pmatrix} V_{inx} \\ V_{iny} \end{pmatrix} = M\begin{pmatrix} I_{mx} \\ I_{my} \end{pmatrix} \quad (4)$$

In the case of MEMS vibratory gyroscopes (4) is modified as:

$$\begin{pmatrix} I_{mx} \\ I_{my} \end{pmatrix} = M^{-1}\begin{pmatrix} V_{inx} \\ V_{iny} \end{pmatrix} \quad (5)$$

The output electrode of the gyroscope is connected to a transimpedance amplifier (TIA). The TIA gain is a complex number, and it amplifies the motional current and it might induce a phase shift in the output voltage. Considering the capacitive feedthrough from the drive voltages, the output voltages can be written as:

$$\begin{pmatrix} V_{outx} \\ V_{outy} \end{pmatrix} = \begin{pmatrix} I_{mx} + I_{x_{fdth}} \\ I_{my} + I_{y_{fdth}} \end{pmatrix}.TIA_{gain} \quad (6)$$

where $I_{x_{fdth}}$ and $I_{y_{fdth}}$ are feedthrough currents seen at the output electrodes of the drive and of the sense modes which are calculated using:

$$\begin{aligned} I_{x_{fdth}} &= jC_{p_{1D}}2\pi f\, V_{inx} + jC_{p_{1s}}2\pi f\, V_{iny} \\ I_{y_{fdth}} &= jC_{p_{2D}}2\pi f\, V_{inx} + jC_{p_{2s}}2\pi f\, V_{iny} \end{aligned} \quad (7)$$

where $C_{p_{1D}}$ is capacitive connection between the input and the output of the drive mode, $C_{p_{1s}}$ is the capacitive connection between the input of the sense mode and the output of the drive mode, $C_{p_{2s}}$ is the capacitive connection between the input and the output of the sense mode, and $C_{p_{2D}}$ is the capacitive connection between the input of the drive mode and the output of the sense mode.

The equivalent electrical model for the drive and the sense mode is presented in Fig. 3.

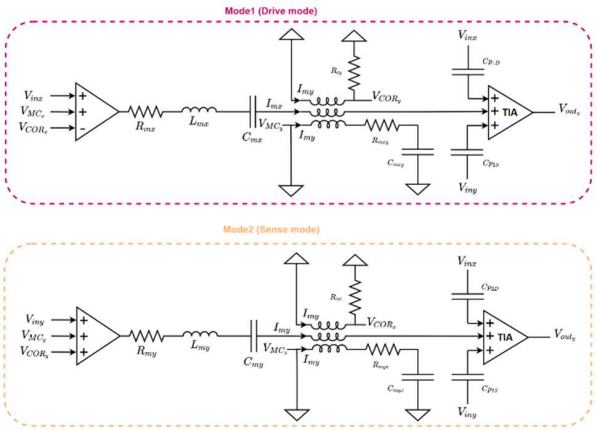

Fig. 3. Equivalent electrical circuit schematics for the drive and the sense modes of a MEMS gyroscope.

IV. Results

A. Open loop frequency sweep

To fit the open loop frequency sweep response using the electrical model, the feedthrough capacitances are extracted in between the ports by applying a zero-bias voltage on the MEMS gyroscope. The RLC components of the drive and of the sense mode are extracted using the response obtained by applying the drive voltage on one electrode and by sensing from another electrode: the pair of electrodes is aligned to the drive mode in the case of the drive mode and to the sense mode in the case of the sense mode. The mechanical crosstalk (RC) from the drive to the sense mode can be estimated by driving the electrode aligned to the drive mode and sensing from the electrode aligned to the sense mode. Similarly, the mechanical crosstalk (RC) from the sense to the drive mode can be estimated by driving the electrode aligned to the sense mode and sensing from the electrode aligned to the drive mode. Finally, both modes are actuated and sensed to fine tune the system.

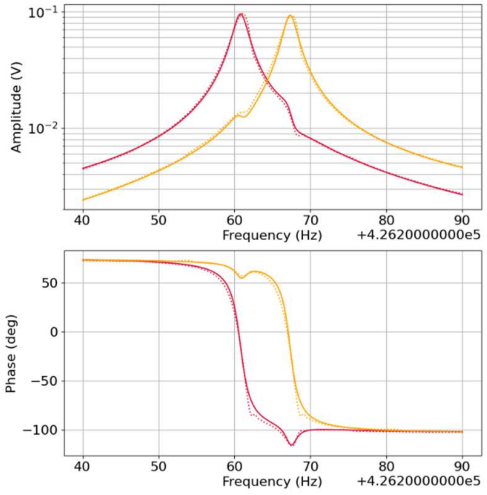

(a)

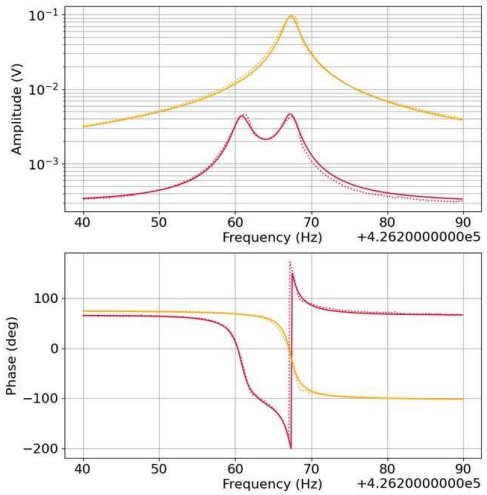

(b)

Fig. 4. Comparison of measured (dotted line) and simulated (continuous line) frequency sweep response of the drive (yellow line) and sense (red line) modes of the gyroscope when: a) both the drive and sense mode actuated with the same signal b) only the input of the drive mode is actuated.

Fig. 4a displays the experimental measurement results of an open loop frequency sweep and the fitted graph using the parameters obtained from the model while driving both the drive and the sense mode; Fig. 4b shows the results while driving only the drive mode.

B. Rate table measurements

The rate table measurements are done to calibrate the Coriolis component which is linear in this model. The device is operated in open-loop sense mode. The resonance tracking of the drive mode is implemented along with AGC to keep the mechanical amplitude of the drive mode constant using a PID controller which compares and regulates the drive mode amplitude to a setpoint. The phase rotator (a_{re}) is adjusted to ensure that the X-component is the quadrature output, and the Y-component is the Coriolis output.

Fig 5. shows the measured and simulated sense mode amplitude and phase for different values of the angular velocity (Ω_z). In order to show the linearity of the Coriolis component of the sense output versus the angular speed, the sense output is plotted in a X-Y representation (Fig 6), where X represents the quadrature component and Y the Coriolis component of the sense response. Fig 6. shows that the variation of the quadrature component is negligible (ΔV=3.5 mV), while the Coriolis component changes (ΔV=200 mV) with the angular speed in alignment with the model.

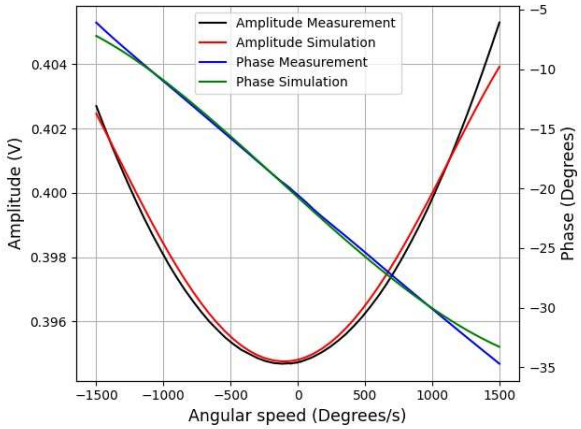

Fig. 5. Measured and simulated sense mode amplitude and phase with respect to change in angular velocity.

The fitting works for angular rates in the order of 100s of deg/s but starts deviating when it is bigger than 1000 deg/s, showing the need to include a higher order term in the model.

A MEMS gyroscope is often operated in a force-to-rebalance (FTR) mode [4] for extended measurement bandwidth and dynamic range. The DRTU can be adapted to set up two additional control loops to null the quadrature and Coriolis components in this configuration. The model can be extended to include these additional circuit blocks for a FTR implementation.

The validation of FTR measurements with the model will be the subject of future investigations.

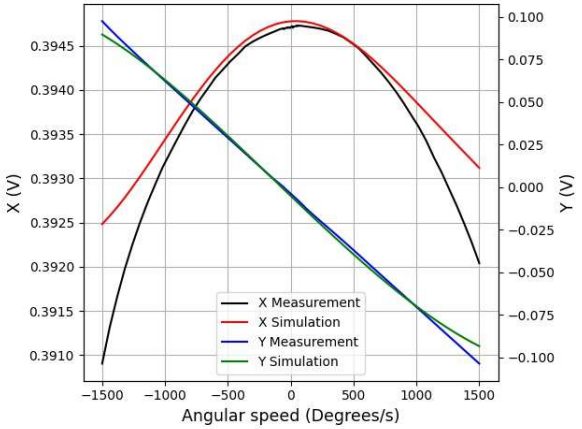

Fig. 6. Measured and simulated quadrature (X) and Coriolis (Y) components of the sense mode with respect to change in angular velocity.

V. Conclusions

This paper presents a linear electrical equivalent model for a MEMS Coriolis Vibratory Gyroscope using a 4-port system. The model is experimentally validated through open-loop gyroscopic measurements conducted on microfabricated quatrefoil suspension gyroscope prototypes. Good alignment is seen between the experimentally measured frequency response and the results of the model. The rate table measurements of the open-loop operation of the gyroscope also align well with the predictions of the model.

The model described in this paper can be further extended to include nonlinear effects and also integrate models of the interface and control electronics. This model can then be applied to identify the basis for performance limitations and optimize future system design.

References

[1] D. D. Lynch. “Coriolis vibratory gyros,” In *Symposium Gyro Technology*, DEUTSCHE GESELLSCHAFT FUER ORTUNG UND NAVIGATION, pp. 1.0–1.14. 1998.

[2] A. Mustafazade et al., “A vibrating beam MEMS accelerometer for gravity and seismic measurements,” Scientific reports, 10(1), p.10415.

[3] M. Parajuli, G. Sobreviela and A. A. Seshia, "A Silicon MEMS Quatrefoil Suspension Gyroscope," in *Journal of Microelectromechanical Systems*, vol. 32, no. 5, pp. 416-425, Oct. 2023

[4] M. Parajuli *et al*., "Closed-Loop Operation of a High-Q Silicon MEMS Quatrefoil Suspension Gyroscope," *2024 IEEE 37th International Conference on Micro Electro Mechanical Systems (MEMS)*, Austin, TX, USA, 2024, pp. 895-898

[5] H. A. C. Tilmans, "Equivalent circuit representation of electromechanical transducers: I. Lumped-parameter systems", *J. Micromechanics and Microengineering*, vol. 6, pp. 157, 1996.

[6] H. A. C. Tilmans, "Equivalent circuit representation of electromechanical transducers: II. Distributed-parameter systems", *J. Micromechanics and Microengineering*, vol. 7, pp. 285-309, 1997.

[7] H. Zhang, C. Weiping, Y. Liang, and F. Qiang,"An Interface ASIC Design of MEMS Gyroscope with Analog Closed Loop Driving," *Sensors* 23, no. 5: 2615, 2023.